Journal of Energy Storage 50 (2022) 104537

Contents lists available at ScienceDirect

Journal of Energy Storage

journal homepage: www.elsevier.com/locate/est

Research papers

A fractional-order model for calendar aging with dynamic storage conditions

Juan Antonio López-Villanueva [a,b,*], Pablo Rodríguez Iturriaga [a], Salvador Rodríguez-Bolívar [a,b]

[a] Department of Electronics and Computer Technology, University of Granada, Facultad de Ciencias, Campus de Fuentenueva, Granada, 18071, Spain
[b] CITIC, University of Granada, Periodista Rafael Gomez Montero, 2, Granada, 18014, Spain

ARTICLE INFO

Keywords:
Lithium-ion battery
Calendar aging
Dynamic conditions
Fractional order

ABSTRACT

Due to the increasing importance of lithium-ion batteries in electric vehicle and renewable energy applications, battery aging is a subject of intense research. Although many laboratory experiments are performed under well-controlled static conditions, batteries are stored and operated under varying conditions of temperature and state of charge in their real-life performance, so that a suitable model for predicting the effects of calendar aging in lithium-ion batteries with dynamic conditions is highly desirable. In this paper, we review previous models to calculate capacity loss due to calendar aging under variable temperature and state-of-charge conditions according to experimentally observed power-law behavior, and propose a novel model based on fractional calculus. To validate the new model, we compare its predictions with experimental results showing that it can reproduce the non-monotonic behavior that is observed when the state of charge or the temperature change significantly. This is an interesting application of fractional calculus since this characteristic is not obtained with non-fractional models.

1. Introduction

Lithium-ion (Li-ion) batteries have been a major breakthrough in electrochemical energy storage [1]. Given their importance in present and future applications, the 2019 Nobel Chemistry Prize has been awarded to some of their pioneers [2]. But despite these important advances, the long-term health of a battery remains a concern [3], and its aging characterization and understanding is a subject of intense research [4–6]. Upon closer examination, two components are usually distinguished in battery aging. One of them is the fading of battery performance observed over time in the absence of electric current, known as calendar aging [4,7,8]; the other one is the degradation that occurs when a charge and discharge current is applied [9,10], known as cycle aging. In a cycled operation, calendar aging mechanisms may also be present, so that cycle and calendar aging are coupled and there may be no simple way to quantify the contribution of each mechanism to overall degradation [11]. One possibility is to switch between calendar and cycle models [12]. Another option is to subtract the effects of calendar from total aging to decouple them from pure cycling outcome [13], but this requires modeling calendar aging under the dynamic conditions that occur while the battery cell is cycled.

Calendar aging is known to be strongly influenced by temperature and state of charge (SOC), as well as other factors such as the chemical composition and structure of the positive and negative electrodes [4]. Its main effects are a loss of battery capacity and an increase in the internal resistance. Capacity fade due to calendar aging is often attributed to losses of Li ions to the solid–electrolyte interphase (SEI) of graphite anodes, and is mainly dependent on the electrochemical potential of the anode at each state of charge. Resistance rise may also be related to the increase in the width of the passivation layer [14]. As these two effects, capacity fade and resistance increase, are assumed to be correlated [15–17], this article focuses on modeling capacity loss.

Two types of models have previously been proposed to model battery aging phenomena, known as physical models [18] and empirical models [19], although sometimes the parameters used in the empirical models have a physical justification [20] and are called semiempirical [10,13,21,22]. Broussely et al. [19] experimentally observed a quadratic dependence of the storage time on the capacity loss in different types of Li-ion batteries, and Bloom et al. [8] fitted the area specific impedance and power fade data to a general thermally activated power-law equation proportional to t^z, with $z = 1/2$. This power-law dependence has been used by many authors since then, with an exponent equal to or close to 0.5 [8,12,13,21–27], although other authors proposed $z = 0.75$ or close to it [16,28,29]. These time dependences have been reviewed by Gasper et al. [30]. The power dependence is multiplied by a factor that depends on the state of charge and the temperature. Schmalstieg et al. [16] proposed an Arrhenius-based semiempirical model, and Petit et al. [12] developed an empirical capacity loss model to evaluate the effects of SOC and temperature. Redondo-Iglesias et al. [11,26] adopted a semiempirical

* Corresponding author at: CITIC, University of Granada, Periodista Rafael Gomez Montero, 2, Granada, 18014, Spain.
E-mail address: jalopez@ugr.es (J.A. López-Villanueva).

https://doi.org/10.1016/j.est.2022.104537
Received 20 January 2022; Received in revised form 7 March 2022; Accepted 26 March 2022
Available online 18 April 2022

approach based on the Eyring acceleration instead of using the Arrhenius dependence. All these semiempirical models include functional dependencies with physical justification and some free parameters to be determined by fitting to experimental data.

In calendar aging laboratory experiments, ambient temperature and state of charge are generally chosen and maintained except in brief periods of time in which the capacity and resistance changes are measured. This is repeated for several choices of these parameters in order to obtain the functional dependence on them [13,16,24]. But in normal operation a battery operates under dynamic conditions [4,25]. Therefore, various models have been developed in an attempt to forecast the calendar life of Li-ion batteries under varying storage conditions. The model proposed in [7] allows to simulate the degradation induced by storage under non-static conditions using the derivative form. Refs. [12,13,17,21,22,31,32] also presented models to analyze the impact of calendar aging under varying conditions. Data-based models has also been developed to continuously learn from streaming data [33]. The Gaussian process method was proposed and applied for this purpose [5,34]. However semiempirical modeling is the most widely used method for this goal and we will restrict ourselves to analyzing and proposing semiempirical approaches based on power-law dependency in this article.

Fractional calculus has been widely used to model the electric behavior of batteries and supercapacitors, relating voltage and current both in the frequency and time domains [35–37]. In a more general way, physical systems described by a power law can be represented by fractional order models [38]. In this article we make use of the fact that calendar aging has shown a power law dependence with time to propose a new fractional-order aging model. This new model has two fundamental advantages. The first one is related to the behavior of the calendar aging under dynamic conditions, as this new model produces the same results than the other semiempirical models in the case of static storage conditions but shows interesting quantitative and qualitative differences under dynamic storage conditions. The second one is related to the dependence of the calendar aging on all the previous history experienced by the battery. Previous works have highlighted the dependence of calendar aging on its history, addressing it by making use of Gaussian process regression since output can be predicted using this method to learn the underlying mappings among all input terms including the historical capacity data vector [34]. In the model we present in this article, the known fact that the result of fractional-order differential equations depends on the whole history [39,40] is incorporated.

Our model will assume that calendar aging depends on the state of charge and temperature during battery storage. These dependences have been carefully studied by previous authors [8,13,22–24]. However, the goal of this article is not to study these dependences in detail, but to discuss how to consider them when storage conditions are changed dynamically. Some previously used models will be discussed, and fractional calculus methods will be employed to propose a new one that can account for experimental features not predicted by previous models.

The outline of this article is as follows. Section 2 briefly reviews some previous semiempirical models for predicting calendar aging under dynamic conditions. The new fractional-order model is described in Section 3. A comparison of both the non-fractional and the fractional-order models with experimental results is shown in Section 4. The effect of pre-aging due to storage before the measurement of capacity fade is discussed in Section 5, and finally some conclusions are drawn in Section 6.

2. Empirical calendar models under dynamic conditions

We start with the power-law dependence of the capacity loss proposed by many authors [8,13,16,21,23–25,28]. If we define the capacity loss as

$$L(t) = \frac{Q_0 - Q(t)}{Q_0}, \tag{1}$$

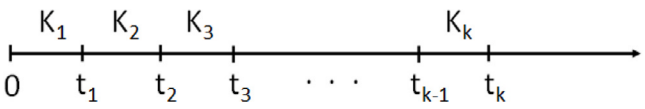

Fig. 1. Discretized time under varying storage conditions. Values of $K(SOC,T)$ are assumed to be constant within each subinterval.

where Q_0 is the initial capacity and $Q(t)$ is the capacity at time t, then the semiempirical equation is written as

$$L(t) = K(SOC,T)\cdot t^z\ , \tag{2}$$

where the function $K(SOC,T)$ is actually assumed to be a constant in the time interval $(0,t)$. It can be factored into a function of temperature multiplied by a function of the state of charge, where an Arrhenius-type dependence is assumed for the temperature [8,23], and the state-of-charge dependence has often been written in terms of the cell potential as a Tafel-type function [13,22,24]. We assume in this section that this function of SOC and T is known, since it has been obtained from calendar aging experiments performed under static conditions in which these magnitudes are well controlled, but its values can still be used when the state of charge and the temperature change under dynamic conditions.

We will discretize the time in a series of subintervals $[0,t_1]$, $(t_1,t_2]$, $(t_3,t_2]$, …, $(t_{k-1},t_k]$, and we will approximate the function $K(SOC,T)$ by a constant value within each of them, with values $K_1, K_2, K_3, \ldots, K_k$, respectively, as shown in Fig. 1.

The length of the time subintervals can be arbitrary if the storage conditions are changed in a stepwise form, but the procedure of this section can also be applied in case of a continuous variation of the storage conditions if the time step is small enough.

In order to extend the power-law result to the case of dynamic operating conditions, a more general equation that gives Eq. (2) as its solution under static conditions, but can also be used under dynamic conditions, has been sought. For this, several authors have considered Eq. (2) as the solution of

$$\frac{dL}{dt} = z\ K(SOC,T)\ t^{z-1}, \tag{3}$$

and they have assumed that Eq. (3) can also be applied when function K depends implicitly on time through $SOC(t)$ and $T(t)$ [12,13,21,31,32]. This can be done in two ways, giving rise to the models we call Model 1 and Model 2, respectively.

2.1. Model 1

Eq. (3) can be integrated directly keeping the explicit dependence on time in the right-hand side, as proposed by [31] and applied by other authors [13,21]. The result is

$$L(t) = z\int_0^t K[SOC(\tau),T(\tau)]\tau^{z-1}d\tau \tag{4}$$

The capacity loss at time t_k, when dividing the interval $[0,t_k]$ into its subintervals according to Fig. 1, is

$$L(t_k) = \sum_{j=1}^{k} K_j\cdot(t_j^z - t_{j-1}^z), \tag{5}$$

with $t_0 = 0$.

2.2. Model 2

The second procedure was used by Petit et al. [12] and other authors [32]. Before integrating Eq. (3), the explicit time dependence can be eliminated by substituting it according to Eq. (2)

$$t = \left(\frac{L}{K}\right)^{\frac{1}{z}}, \tag{6}$$

thus obtaining

$$\frac{L^{\frac{1}{z}-1}}{z}\frac{dL}{dt} = K^{\frac{1}{z}}, \tag{7}$$

which can be integrated arriving at

$$[L(t)]^{\frac{1}{z}} = \int_0^t [K(SOC(\tau),T(\tau))]^{\frac{1}{z}} d\tau. \tag{8}$$

By dividing again the interval $[0,t_k]$ into its subintervals according to Fig. 1, the result for Model 2 is

$$L(t_k) = \left[\sum_{j=1}^{k} K_j^{\frac{1}{z}} \cdot (t_j - t_{j-1})\right]^z \tag{9}$$

This same result has been obtained by Hahn et al. [22] in a somewhat different way. If the value of K in the interval $(t_{k-1},t_k]$ is K_k, they defined an "equivalent" time t^*_{k-1} so that the capacity loss at t_{k-1} could be written as

$$L(t_{k-1}) = K_k \cdot (t^*_{k-1})^z. \tag{10}$$

Time t^*_{k-1} therefore includes the effect of all previous values of K different from K_k. The capacity loss at t_k, after adding the contribution of the interval $(t_{k-1},t_k]$, is

$$L(t_k) = K_k \cdot [t^*_{k-1} + (t_k - t_{k-1})]^z \tag{11}$$

Substituting t^*_{k-1} from Eq. (10) in Eq. (11), the result is

$$L(t_k) = [(L(t_{k-1}))^{\frac{1}{z}} + K_k^{\frac{1}{z}} \cdot (t_k - t_{k-1})]^z, \tag{12}$$

Applying Eq. (12) to the successive subintervals, the result given in Eq. (9) is also obtained.

3. Fractional-order model

Another possibility of eliminating the dependence on time in the derivative of $L(t)$ is given by fractional calculus. The non-integer derivative of order z of the capacity loss, by assuming constant K in Eq. (2), is [39,40]

$$\frac{d^z L(t)}{dt^z} = \Gamma(z+1)K(SOC,T), \tag{13}$$

where $\Gamma(z)$ is the Gamma function [40]. We propose to generalize Eq. (13) to a case with variable K, and integrate it with the Riemann–Liouville definition of the fractional integral of order z, $D^{-z}f(t)$, defined as [40]

$$D^{-z}f(t) = \frac{1}{\Gamma(z)}\int_0^t \frac{f(\tau)}{(t-\tau)^{1-z}} d\tau. \tag{14}$$

Using definition (14), and the relationship

$$\frac{\Gamma(z+1)}{\Gamma(z)} = z, \tag{15}$$

the result is

$$L(t) = z\int_0^t \frac{K[SOC(\tau),T(\tau)]}{(t-\tau)^{1-z}} d\tau. \tag{16}$$

The interval $[0,t_k]$ can also be subdivided into its subintervals according to Fig. 1, thus obtaining at time t_k

$$L(t_k) = z\sum_{j=1}^{k} K_j \int_{t_{j-1}}^{t_j} \frac{d\tau}{(t_k-\tau)^{1-z}}, \tag{17}$$

and the final result for the fractional-order model is as follows

$$L(t_k) = \sum_{j=1}^{k} K_j \cdot \left[(t_k - t_{j-1})^z - (t_k - t_j)^z\right]. \tag{18}$$

Now we have three different models to account for the capacity loss produced by calendar aging with non-static storage conditions, specifically the two models adapted from the previous literature, given in Eqs. (5) and (9), and the model proposed in this article given by Eq. (18). The three expressions will provide the same result if $k = 1$ (static conditions). In case of varying conditions, they will result in quantitative differences, but there is also a remarkable qualitative distinction of the fractional-order model with respect to the other two. Whereas in Eqs. (5) and (9) any new time interval produces an increase in the capacity loss, and hence these models are monotonic, Eq. (18) is not necessarily monotonic since the last time instant, t_k, appears in all the terms of the sum so that there is an influence of all previous storage conditions also in the contribution of the last interval. This memory of the whole history is a feature of fractional calculus, and it has a relevant impact on the results.

To illustrate the different behavior of the fractional and non-fractional models in a practical case, a model of the function $K(SOC,T)$ is required. Since the aim of this article is to discuss how to deal with non-static storage conditions and not to discuss different possibilities for $K(SOC,T)$, we have chosen the semiempirical model by Schimpe et al. [13], detailed in Appendix. As an example, we have compared the three models of Eqs. (5), (9) and (18) by applying them to the variable profiles used by Sarasketa-Zabala et al. in [25] with LFP li-ion battery cells. The exponent $z = 0.5$, the activation energy of the Arrhenius term and the dependence on the state of charge expressed in terms of the anode potential in [13] have been maintained. We have also used the default values of the fit parameters in Appendix with the exception of the constant $k_{cal,Ref}$ that has been chosen in the range $4.6\cdot10^{-4} - 6.6\cdot10^{-4}h^{-0.5}$. The value of this constant in [13] was obtained by fitting the experimental results of the capacity loss measured under static conditions, but although a constant value can be assumed for a given cell, results for the different cells fitted individually may show some variations since they are not exactly identical. The result for the temperature profiles of Fig. 14-(a) to (c) of [25] is shown in Fig. 2. The different quantitative behavior of the three models can be observed, and the non-monotonic behavior of the fractional-order model is apparent in some cases, notably when the storage conditions change from the more aggressive elevated temperatures maintained for long times to significantly lower values, while a monotonic behavior is observed with less abrupt changes. We will discuss this non-monotonic behavior in next Section by fitting several experimental sets of results.

4. Comparison with experimental results

In order to analyze the behavior of the three semiempirical models that we are considering in this paper and compare them with experimental results, a set of experimental data taken at a variety of values of state of charge and temperature, for the same cell, is desirable. We have used in this article two recent sets of experimental data with the required characteristics obtained from Refs. [5,32]. As mentioned above, the semiempirical model by Schimpe et al. [13], detailed in Appendix, which is quite similar to that used by other authors [22], has been used to model the dependences of $K(SOC,T)$. However, we have chosen now as fitting parameters the exponent z, and parameters α, k_0, and $k_{cal,Ref}$, described in Appendix, instead of using the default values provided in Ref. [13].

In the search for the agreement with the experimental results, two objective magnitudes will be minimized, (1) the average relative error given by

$$\overline{\epsilon_{rel}} = \frac{1}{N}\sum_{j=1}^{N}\left[\frac{|\,L_j^{model} - L_j^{exp}\,|}{|\,L_j^{exp}\,|}\right], \tag{19}$$

and (2) the average root–mean–square error divided by the average of the experimental set values, obtained according to

$$\overline{\epsilon_{rms}} = \frac{\sqrt{\sum_{j=1}^{N}\left[L_j^{model} - L_j^{exp}\right]^2}}{\sum_{j=1}^{N}|\,L_j^{exp}\,|}, \tag{20}$$

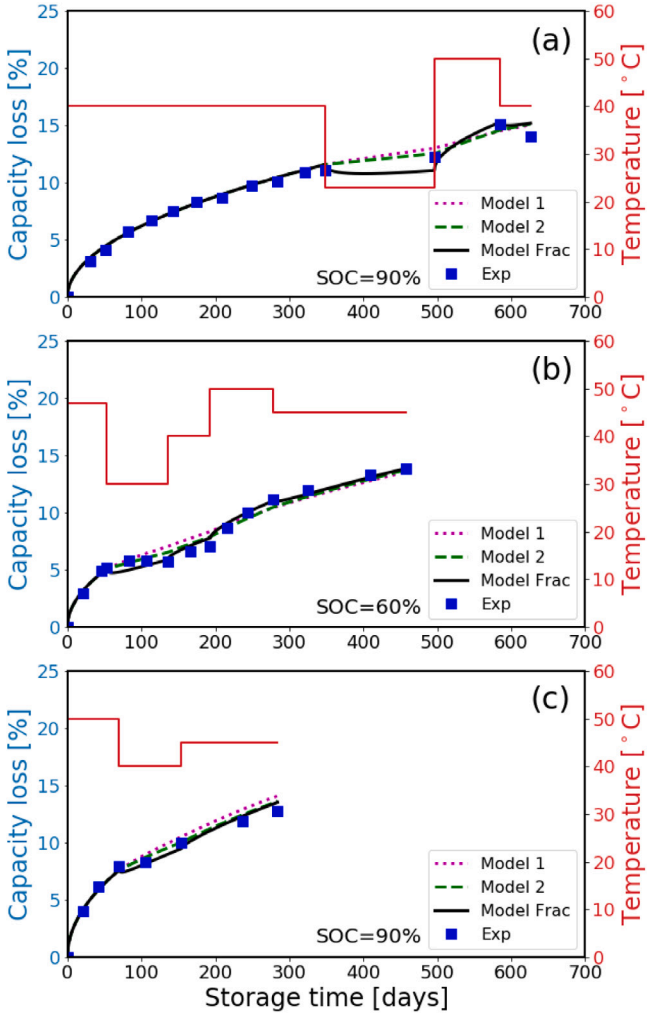

Fig. 2. Temperature profile and capacity loss due to calendar aging predicted by semiempirical power-law models under dynamic conditions for three different tests used in Ref. [25]. A non-monotonic behavior is observed with the fractional-order model in some cases.

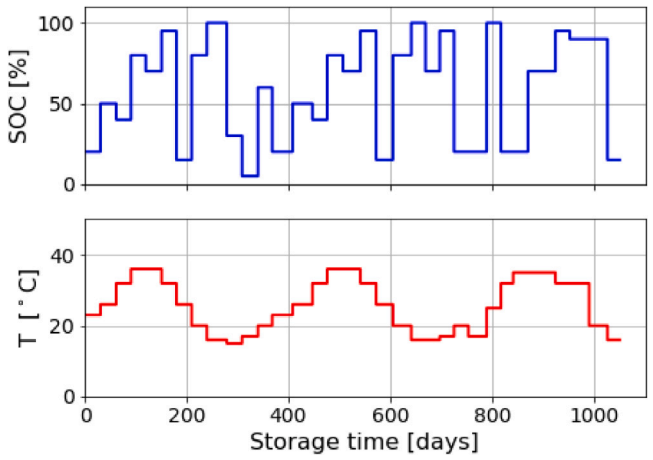

Fig. 3. Profiles of SOC and T used by Lucu et al. [5], used in this article to compare the experimental capacity loss due to calendar aging with results predicted by semiempirical power-law models.

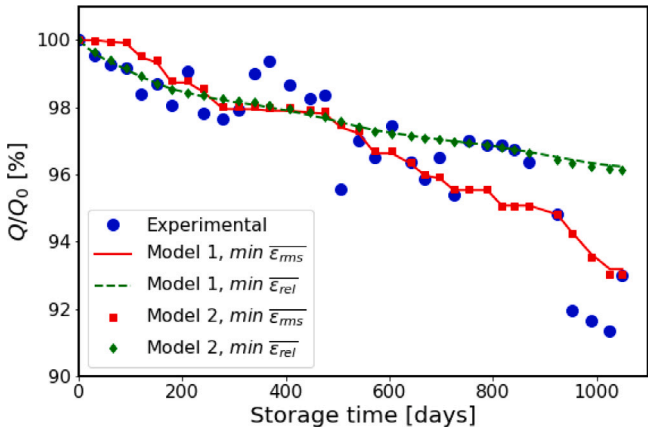

Fig. 4. Experimental results for the capacity from Lucu et al. [5] and approximations with Models 1 and 2 obtained by minimizing $\overline{\epsilon_{rel}}$ and $\overline{\epsilon_{rms}}$.

where L_j^{model} are the values of capacity loss provided by the model, and L_j^{exp} are the experimental capacity losses.

The two types of error provide different information. The average relative error gives more weight to the points with the lowest denominator, which are those measured at the beginning of the curve when the capacity loss is closer to zero. The average root–mean–square error is divided by the average capacity loss and is thus affected by the whole curve, with no privilege to any part of it. This will have noticeable consequences in the resulting fit.

4.1. Data from Lucu et al. [5]

The first data set has been provided by Lucu et al. [5]. These data were measured in a 20 Ah Lithium Nickel–Manganese–Cobalt (NMC 4:4:2) cathode-based pouch cell with a graphite anode and were obtained under a wide variety of storage conditions that were changed every month over three years. The state of charge and temperature profiles taken from Ref. [5] are shown in Fig. 3.

Although Schimpe et al. [13] obtained their $K(SOC, T)$ model for LFP cells, we have initially used it here with NMC cells since it is expressed in terms of the negative electrode potential, which is graphite in the two types of cells. However, the cell differences will provide different parameter values. The result of the relative capacity with respect to the initial capacity ($(1-L(t))\times 100$) obtained with the Models 1 and 2 is shown in Fig. 4 together with the experimental results. The modeled curves correspond to the minimization of the two types of errors defined in Eqs. (19) and (20), and show the expected behavior, with the curve for minimum $\overline{\epsilon_{rel}}$ closer to the experimental data for low storage times but more distant at high storage-time values. The values of the parameters obtained in the fit are shown in Table 1.

The results obtained with Models 1 and 2 are almost coincident, although they have been achieved with different parameters values as observed in Table 1. The high value of the exponent z obtained in the minimization of $\overline{\epsilon_{rms}}$ is noteworthy, which shows that the time dependence is almost linear for long storage times according to these models.

The curves obtained with the fractional-order (FO) model, together with the experimental data, are shown in Fig. 5, where the results for the minimization of the two types of errors is also shown. The values of the parameters obtained in the fit are shown in Table 1 as well.

Both quantitative and qualitative differences can be observed between FO model and Models 1 and 2. Both the average relative error and the average root–mean–square error are smaller with the FO model with a z value close to 0.5 in this case, but even more significant here is that, although the experimental results are not exactly reproduced, the fractional order model shows the fluctuations observed in the experimental behavior, while the Models 1 and 2 are always monotonic and cannot predict such experimental fluctuations.

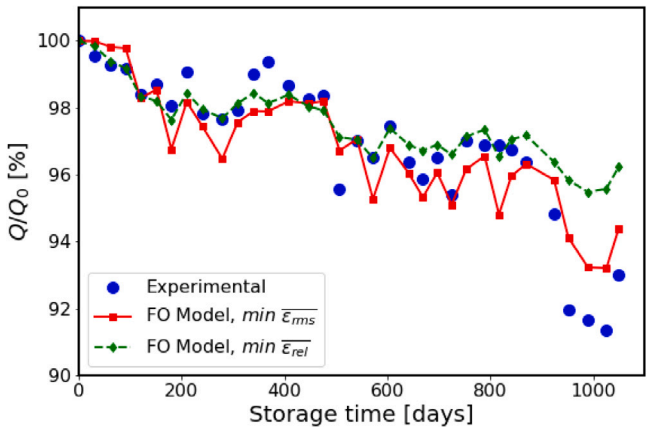

Fig. 5. Experimental results for the capacity from Lucu et al. [5] and approximations with the fractional-order model obtained by minimizing $\overline{\epsilon_{rel}}$ and $\overline{\epsilon_{rms}}$.

Table 1
Values of the parameters for the best agreement with the experimental results of [5].

Objective	z	α	k_0	$k_{cal,Ref}$ $[h^{-z}]$	ϵ_{rel} [%]	ϵ_{rms} [%]
Model 1, ϵ_{rel}	0.58	0.042	0.13	$9.1 \cdot 10^{-5}$	36.5	–
Model 1, ϵ_{rms}	0.95	1.728	0.01	$1.0 \cdot 10^{-6}$	–	5.90
Model 2, ϵ_{rel}	0.63	0.036	0.04	$6.0 \cdot 10^{-5}$	35.9	–
Model 2, ϵ_{rms}	1.00	1.890	0.00	$5.0 \cdot 10^{-7}$	–	5.82
FO Model, ϵ_{rel}	0.50	0.540	0.06	$1.82 \cdot 10^{-4}$	31.4	–
FO Model, ϵ_{rms}	0.54	1.700	0.00	$5.15 \cdot 10^{-5}$	–	5.48

Table 2
Values of the parameters for the best agreement with the experimental results of [32].

Objective	z	α	k_0	$k_{cal,Ref}$ $[h^{-z}]$	ϵ_{rms} [%]
Model 1, ϵ_{rms}	0.54	1.146	0.097	$1.09 \cdot 10^{-4}$	2.68
Model 2, ϵ_{rms}	0.66	0.956	0.00	$3.02 \cdot 10^{-5}$	2.50
FO Model, ϵ_{rms}	0.69	0.573	0.046	$3.61 \cdot 10^{-5}$	1.49

4.2. Data from Mingant et al. [32]

The inability of Model 2 to represent the non-monotonic behavior of the experimental data has been recognized by Mingant el al. [32]. They have also used NMC cells and have provided experimental results obtained by alternating the SOC while storing the battery cells. The experimental data have been obtained storing the battery cell at a temperature of 45 °C and varying the state of charge in a sequence 30%, 80%, 80%, 30%, 80%, 80%, etc. They claim that the experimental data show regeneration of the capacity at 30% of SoC after having stored the battery cells at an SOC equal to 80%, and realized that this phenomenon is not considered by Model 2, since it leads to a monotonic equation. However, the fractional-order model proposed in this article can actually account for this regeneration. We have also compared the experimental data provided in Figure 9 of Ref. [32] with the predictions of the three models. The result is shown in Figs. 6, for Models 1 and 2, and in Fig. 7 for the fractional-order model. The values of the parameters obtained in the fit to the experimental results are shown in Table 2.

It can be observed that, once the suitable parameter values are chosen for each model, the approximations obtained with Models 1 and 2 are reasonably satisfactory and almost coincident. However, none of them is capable of predicting the non monotonic behavior. The fractional-order model actually predicts the non-monotonic behavior and produces a better agreement with a smaller error although we have used the same fitting parameters with all three models.

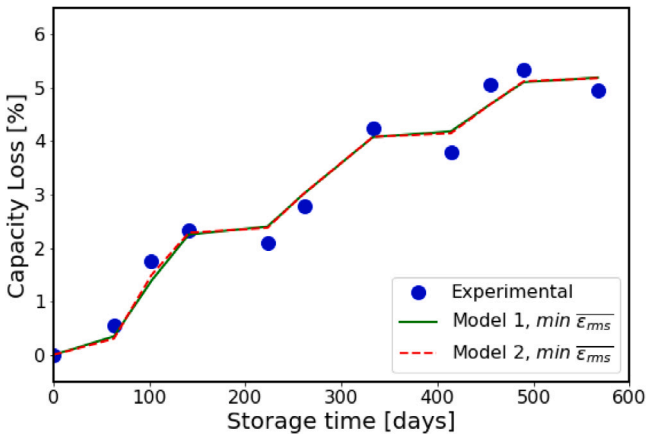

Fig. 6. Experimental results for the capacity loss from Mingant et al. [32] and approximations with models 1 and 2.

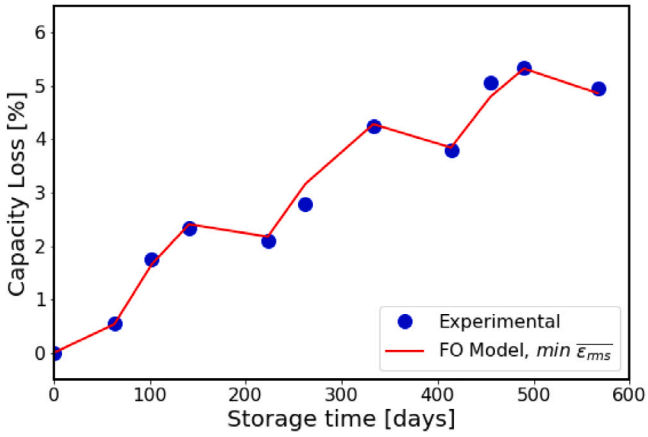

Fig. 7. Experimental results for the capacity loss from Mingant et al. [32] and approximation with the fractional-order model.

5. Effect of initial aging

Finally, once we have demonstrated the good behavior of the fractional-order model, as a corollary we will apply it in this Section to the case of the existence of a storage period prior to the measurement of the capacity fade. Since calendar aging depends on the whole history of the battery cell, the storage-time interval from manufacture to the start of measurement may have some influence on the results. To analyze this, we now assume that the cell was manufactured at $t = 0$, and the capacity at the beginning of its life is Q_{bol}. We also assume that the battery has been stored for a time t_0 prior to the measurement with an effective value of K equal to K_0, so that the capacity at $t = t_0$ is Q_0. After t_0 the capacity fade is measured periodically with controlled storage conditions up to time t, so that $K = K_1$ in the interval $(t_0, t]$, where the K_1 value has been set up by the experimenter. Hence, the capacity loss at time t is

$$L(t) = \frac{Q_{bol} - Q(t)}{Q_{bol}}, \tag{21}$$

so that

$$L_0 = \frac{Q_{bol} - Q_0}{Q_{bol}}, \tag{22}$$

is the capacity loss at the start of the measurement.

But the experimenter has taken Q_0 as the initial capacity and measures

$$L^*(t') = \frac{Q_0 - Q(t)}{Q_0}, \tag{23}$$

where

$$t' \equiv t - t_0, \tag{24}$$

is the observation time.

By combining Eqs. (21) and (22) to eliminate Q_{bol}, and substituting Q_0 in Eq. (23), we obtain

$$L^*(t') = \frac{L(t) - L_0}{1 - L_0}. \tag{25}$$

We can calculate $L^*(t')$ with the three models given in Eqs. (5), (9), and (18), by considering only two time intervals, $[0, t_0]$ and $(t_0, t]$. The result is

1. Model 1:

$$L(t) = K_0 \cdot t_0^z + K_1 \cdot (t^z - t_0^z) \tag{26}$$

2. Model 2:

$$L(t) = \left[K_0^{\frac{1}{z}} \cdot t_0 + K_1^{\frac{1}{z}} \cdot (t - t_0)\right]^z \tag{27}$$

3. Fractional-order model:

$$L(t) = K_0 \cdot \left[t^z - (t - t_0)^z\right] + K_1 \cdot (t - t_0)^z \tag{28}$$

And by using Eqs. (24), (25), and

$$L_0 = K_0 \cdot t_0^z, \tag{29}$$

we finally obtain:

1. Model 1:

$$L^*(t') = \frac{K_1 \cdot [(t_0 + t')^z - t_0^z]}{1 - L_0} \tag{30}$$

2. Model 2:

$$L^*(t') = \frac{1}{1 - L_0}\left\{\left[L_0^{\frac{1}{z}} + K_1^{\frac{1}{z}} \cdot t'\right]^z - L_0\right\} \tag{31}$$

3. Fractional-order model:

$$L^*(t') = \frac{1}{1 - L_0}\left\{L_0\left[\left(1 + \frac{t'}{t_0}\right)^z - \left(\frac{t'}{t_0}\right)^z - 1\right] + K_1 \cdot (t')^z\right\} \tag{32}$$

The second term in Eqs. (28) and (32) follows the power-law for the observation time, despite the previous aging, while the first term in (28) corresponds to the initial capacity loss multiplied by a function that decays with time. This decay function is similar to the one obtained in the case of the initialization of constant-phase elements in circuit models used to represent the electrical behavior of batteries [41].

The experimenter can evaluate whether Eq. (2) can fit the simulated data. In fact, the results of Eqs. (30), (31), and (32) can be approximated by Eq. (2) with reasonable accuracy but different values of K and z. To show this, we have simulated capacity-loss curves with the three models (Model 1, Model 2, and FO model), by choosing $z = 0.5$ and the $K(SOC, T)$ values provided by the model of Schimpe et al. [13] with its default parameters detailed in Appendix. We have chosen an initial capacity loss of $L_0 = 2.93\%$, which correspond to a pre-aging time interval of $t_0 = 180$ days of storage at $SOC = 60\%$ and $T = 25$ °C. After that, the cell is stored for a measurement time of two years, at $SOC = 80\%$ and $T = 45$ °C which correspond to $K_1 = 1.05 \cdot 10^{-3} h^{-0.5}$. The results provided by Eqs. (30), (31), and (32) for $t > t_0$ ($t' > 0$) are shown in Fig. 8 in symbols. Then, we have tried to fit the simulated results to Eq. (2), obtaining the results shown in solid lines. However, these fitted curves are obtained with $z = 0.79$ and $K = 3.93 \cdot 10^{-5} h^{-0.79}$ for the curve of Model 1, $z = 0.65$ and $K = 2.02 \cdot 10^{-4} h^{-0.65}$ for the curve of Model 2, and $z = 0.58$ and $K_1 = 4.13 \cdot 10^{-4} h^{-0.58}$ for the curve of the fractional-order model. We observe that the values of K and z are different from those used in the simulation. The fitted exponent z is different from the assumed value, $z = 0.5$, but the exponent achieved to fit the result of the fractional-order model shows the smallest deviation. Therefore, the fractional-order model seems to be the least affected by the capacity loss prior to measurement in this respect.

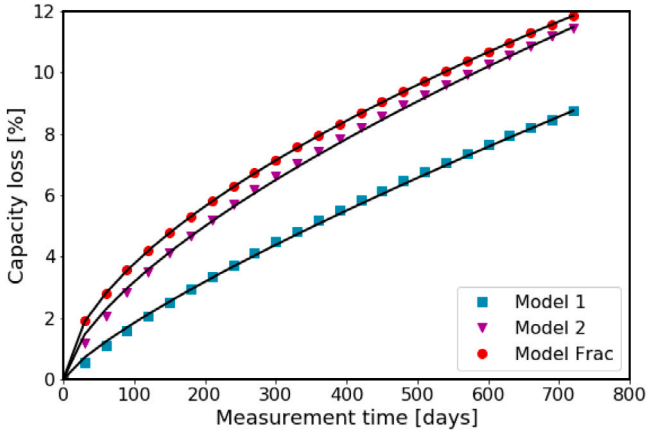

Fig. 8. Capacity loss for a battery cell previously aged in a 2.93%, as a function of time, according to the models in Eqs. (5), (9), and (18). Fit to Eq. (2) in solid lines,.

6. Conclusions

A suitable model to predict the effects of calendar aging in lithium-ion batteries under dynamic storage conditions is highly desirable. Although many laboratory experiments are conducted under well-controlled static conditions in order to analyze the SOC and T dependence of capacity fade and resistance increase, mainly with the state of charge and temperature, these conditions are variable in real life operation. Furthermore, calendar aging mechanisms may also act during cycled operation so that it is necessary to model calendar aging under the dynamic conditions that occur while cycling the battery cell to separate their effects from pure cycle aging.

A model for the capacity fade due to calendar aging under dynamic conditions, based on fractional calculus, has been proposed here. This model is applicable with a suitable semiempirical function that accounts for the dependencies on the state of charge and the temperature. Although some models have been previously proposed in the literature, these models are not totally satisfactory since they are not capable of predicting features such as the non-monotonic behavior which has been observed experimentally. The model proposed here not only provides comparable, even better, accuracy than previous models, but is also capable of predicting the non-monotonic behavior that is observed when the state of charge or temperature are significantly changed. This model has been compared with previous models and has been validated by comparing its prediction with the experimental results. It has also been used to analyze the effects of an aging period previous to the experimental evaluation.

Although we have proposed the fractional-order model without venturing any physical explanation of the application of fractional calculus to this problem, it appears to be an interesting application of fractional calculus, since it not only produces quantitative differences, but also makes qualitatively different predictions than those of the non-fractional models. We consider that its physical significance warrants further investigation.

CRediT authorship contribution statement

Juan Antonio López-Villanueva: Conceptualization, Methodology, Software, Investigation, Writing. **Pablo Rodríguez Iturriaga:** investigation, Writing – review & editing. **Salvador Rodríguez-Bolívar:** Methodology, Software, Investigation, Writing – review & editing.

Declaration of competing interest

The authors declare that they have no known competing financial interests or personal relationships that could have appeared to influence the work reported in this paper.

Acknowledgements

Funding for open access charge: Universidad de Granada / CBUA.

Appendix. Calendar model by Schimpe et al. [13]

This calendar aging model uses the power law with exponent equal to 0.5.

$$L(t) = K(SOC, T)\sqrt{t}. \tag{A.1}$$

However, sometimes we will leave the exponent as a fitting parameter and use Eq. (2) instead. The K constant is modeled as

$$K(SOC, T) = k_{cal,Ref} f_S(SOC) f_T(T), \tag{A.2}$$

with

$$f_S(SOC) = exp\left(\frac{\alpha F(U_{a,ref} - U_a)}{R_g T_{ref}}\right) + k_0 \tag{A.3}$$

and

$$f_T(T) = exp\left(-\frac{E_a}{R_g}\left(\frac{1}{T} - \frac{1}{T_{ref}}\right)\right). \tag{A.4}$$

$E_a = 20592$ J/mol, $R_g = 8.314$ J/(molK) is the universal gas constant, and $F = 96485.3$ C/mol is the Faraday constant.

U_a is the anode voltage. Its values, taken from Safari et al. [42], are obtained according to next equation

$$\begin{aligned} U_a = {} & 0.6379 + 0.5416 \cdot exp(-305.5309 x_a) + 0.044 \cdot tanh\left(-\frac{x_a - 0.1958}{0.1088}\right) - \\ & 0.1978 \cdot tanh\left(\frac{x_a - 1.057}{0.0854}\right) - 0.6875 \cdot tanh\left(\frac{x_a + 0.0117}{0.0529}\right) - \\ & 0.0175 \cdot tanh\left(\frac{x_a - 0.5692}{0.0875}\right) V \end{aligned} \tag{A.5}$$

with $x_a = 8.5 \cdot 10^{-3} + SOC \cdot 0.7715$

The reference potential $U_{a,Ref}$ is set to $U_a(SOC = 50\%) = 0.123$ V.

Schimpe et al. fitted the equation parameters for their experimental data at $T_{Ref} = 298.15$ K obtaining

$\alpha = 0.384$,

$k_0 = 0.142$, and

$k_{cal,Ref} = 3.694 \cdot 10^{-4} h^{-0.5}$

However, these parameter values are modified sometimes in this article to better fit the experimental results.

References

[1] G. Zubi, R. Dufo-López, M. Carvalho, G. Pasaoglu, The lithium-ion battery: State of the art and future perspectives, Renew. Sustain. Energy Rev. 89 (2018) 292–308, http://dx.doi.org/10.1016/j.rser.2018.03.002, URL https://www.sciencedirect.com/science/article/pii/S1364032118300728.

[2] J. Xie, Y.-C. Lu, A retrospective on lithium-ion batteries, Nature Commun. 11 (1) (2020) 2499, http://dx.doi.org/10.1038/s41467-020-16259-9.

[3] Z. Deng, X. Hu, P. Li, X. Lin, X. Bian, Data-driven battery state of health estimation based on random partial charging data, IEEE Trans. Power Electron. 37 (5) (2022) 5021–5031, http://dx.doi.org/10.1109/TPEL.2021.3134701.

[4] M. Dubarry, N. Qin, P. Brooker, Calendar aging of commercial Li-ion cells of different chemistries – A review, Curr. Opin. Electrochem. 9 (2018) 106–113, http://dx.doi.org/10.1016/j.coelec.2018.05.023, URL https://www.sciencedirect.com/science/article/pii/S2451910318300929.

[5] M. Lucu, E. Martinez-Laserna, I. Gandiaga, K. Liu, H. Camblong, W. Widanage, J. Marco, Data-driven nonparametric Li-ion battery ageing model aiming at learning from real operation data – Part A: Storage operation, J. Energy Storage 30 (2020) 101409, http://dx.doi.org/10.1016/j.est.2020.101409, URL https://www.sciencedirect.com/science/article/pii/S2352152X19314215.

[6] M. Lucu, E. Martinez-Laserna, I. Gandiaga, K. Liu, H. Camblong, W. Widanage, J. Marco, Data-driven nonparametric Li-ion battery ageing model aiming at learning from real operation data - Part B: Cycling operation, J. Energy Storage 30 (2020) 101410, http://dx.doi.org/10.1016/j.est.2020.101410, URL https://www.sciencedirect.com/science/article/pii/S2352152X19314239.

[7] S. Grolleau, A. Delaille, H. Gualous, P. Gyan, R. Revel, J. Bernard, E. Redondo-Iglesias, J. Peter, Calendar aging of commercial graphite/LiFePO4 cell – predicting capacity fade under time dependent storage conditions, J. Power Sources 255 (2014) 450–458, http://dx.doi.org/10.1016/j.jpowsour.2013.11.098, URL https://www.sciencedirect.com/science/article/pii/S0378775313019411.

[8] I. Bloom, B.W. Cole, J.J. Sohn, S.A. Jones, E.G. Polzin, V.S. Battaglia, G.L. Henriksen, C. Motloch, R. Richardson, T. Unkelhaeuser, D. Ingersoll, H.L. Case, An accelerated calendar and cycle life study of Li-ion cells, J. Power Sources 101 (2) (2001) 238–247, http://dx.doi.org/10.1016/S0378-7753(01)00783-2.

[9] M. Ecker, N. Nieto, S. Käbitz, J. Schmalstieg, H. Blanke, A. Warnecke, D.U. Sauer, Calendar and cycle life study of Li(NiMnCo)O2-based 18650 lithium-ion batteries, J. Power Sources 248 (2014) 839–851, http://dx.doi.org/10.1016/j.jpowsour.2013.09.143, URL https://www.sciencedirect.com/science/article/pii/S0378775313016510.

[10] J. de Hoog, J.-M. Timmermans, D. Ioan-Stroe, M. Swierczynski, J. Jaguemont, S. Goutam, N. Omar, J. Van Mierlo, P. Van Den Bossche, Combined cycling and calendar capacity fade modeling of a nickel-manganese-cobalt oxide cell with real-life profile validation, Appl. Energy 200 (2017) 47–61, http://dx.doi.org/10.1016/j.apenergy.2017.05.018, URL https://www.sciencedirect.com/science/article/pii/S0306261917305251.

[11] E. Redondo-Iglesias, P. Venet, S. Pelissier, Global model for self-discharge and capacity fade in lithium-ion batteries based on the generalized eyring relationship, IEEE Trans. Veh. Technol. 67 (1) (2018) 104–113, http://dx.doi.org/10.1109/TVT.2017.2751218.

[12] M. Petit, E. Prada, V. Sauvant-Moynot, Development of an empirical aging model for Li-ion batteries and application to assess the impact of Vehicle-to-Grid strategies on battery lifetime, Appl. Energy 172 (C) (2016) 398–407, http://dx.doi.org/10.1016/j.apenergy.2016.0.

[13] M. Schimpe, M.E. von Kuepach, M. Naumann, H.C. Hesse, K. Smith, A. Jossen, Comprehensive modeling of temperature-dependent degradation mechanisms in lithium iron phosphate batteries, J. Electrochem. Soc. 165 (2) (2018) A181–A193, http://dx.doi.org/10.1149/2.1181714jes.

[14] P. Keil, S.F. Schuster, J. Wilhelm, J. Travi, A. Hauser, R.C. Karl, A. Jossen, Calendar aging of lithium-ion batteries, J. Electrochem. Soc. 163 (9) (2016) A1872–A1880, http://dx.doi.org/10.1149/2.0411609jes.

[15] S. Käbitz, J.B. Gerschler, M. Ecker, Y. Yurdagel, B. Emmermacher, D. André, T. Mitsch, D.U. Sauer, Cycle and calendar life study of a graphite|LiNi1/3Mn1/3Co1/3O2 Li-ion high energy system. Part A: Full cell characterization, J. Power Sources 239 (2013) 572–583, http://dx.doi.org/10.1016/j.jpowsour.2013.03.045, URL https://www.sciencedirect.com/science/article/pii/S0378775313004369.

[16] J. Schmalstieg, S. Käbitz, M. Ecker, D.U. Sauer, A holistic aging model for Li(NiMnCo)O2 based 18650 lithium-ion batteries, J. Power Sources 257 (2014) 325–334, http://dx.doi.org/10.1016/j.jpowsour.2014.02.012, URL https://www.sciencedirect.com/science/article/pii/S0378775314001876.

[17] L. Su, J. Zhang, J. Huang, H. Ge, Z. Li, F. Xie, B.Y. Liaw, Path dependence of lithium ion cells aging under storage conditions, J. Power Sources 315 (2016) 35–46, http://dx.doi.org/10.1016/j.jpowsour.2016.03.043, URL https://www.sciencedirect.com/science/article/pii/S0378775316302439.

[18] M. Safari, M. Morcrette, A. Teyssot, C. Delacourt, Multimodal physics-based aging model for life prediction of Li-ion batteries, J. Electrochem. Soc. 156 (3) (2009) A145, http://dx.doi.org/10.1149/1.3043429.

[19] M. Broussely, S. Herreyre, P. Biensan, P. Kasztejna, K. Nechev, R. Staniewicz, Aging mechanism in Li ion cells and calendar life predictions, J. Power Sources 97–98 (2001) 13–21, http://dx.doi.org/10.1016/S0378-7753(01)00722-4, URL https://www.sciencedirect.com/science/article/pii/S0378775301007224 Proceedings of the 10th International Meeting on Lithium Batteries.

[20] S. Khaleghi Rahimian, M.M. Forouzan, S. Han, Y. Tang, A generalized physics-based calendar life model for Li-ion cells, Electrochim. Acta 348 (2020) 136343, http://dx.doi.org/10.1016/j.electacta.2020.136343, URL https://www.sciencedirect.com/science/article/pii/S0013468620307350.

[21] M. Naumann, M. Schimpe, P. Keil, H.C. Hesse, A. Jossen, Analysis and modeling of calendar aging of a commercial LiFePO4/graphite cell, J. Energy Storage 17 (2018) 153–169, http://dx.doi.org/10.1016/j.est.2018.01.019, URL https://www.sciencedirect.com/science/article/pii/S2352152X18300665.

[22] S.L. Hahn, M. Storch, R. Swaminathan, B. Obry, J. Bandlow, K.P. Birke, Quantitative validation of calendar aging models for lithium-ion batteries, J. Power Sources 400 (2018) 402–414, http://dx.doi.org/10.1016/j.jpowsour.2018.08.019, URL https://www.sciencedirect.com/science/article/pii/S0378775318308784.

[23] J. Wang, P. Liu, J. Hicks-Garner, E. Sherman, S. Soukiazian, M. Verbrugge, H. Tataria, J. Musser, P. Finamore, Cycle-life model for graphite-LiFePO4 cells, J. Power Sources 196 (8) (2011) 3942–3948, http://dx.doi.org/10.1016/j.jpowsour.2010.11.134, URL https://www.sciencedirect.com/science/article/pii/S0378775310021269.

[24] M. Ecker, J.B. Gerschler, J. Vogel, S. Käbitz, F. Hust, P. Dechent, D.U. Sauer, Development of a lifetime prediction model for lithium-ion batteries based on extended accelerated aging test data, J. Power Sources 215 (2012) 248–257, http://dx.doi.org/10.1016/j.jpowsour.2012.05.012, URL https://www.sciencedirect.com/science/article/pii/S0378775312008671.

[25] E. Sarasketa-Zabala, I. Gandiaga, L. Rodriguez-Martinez, I. Villarreal, Calendar ageing analysis of a LiFePO4/graphite cell with dynamic model validations: Towards realistic lifetime predictions, J. Power Sources 272 (2014) 45–57, http://dx.doi.org/10.1016/j.jpowsour.2014.08.051, URL https://www.sciencedirect.com/science/article/pii/S0378775314013068.

[26] E. Redondo-Iglesias, P. Venet, S. Pelissier, Eyring acceleration model for predicting calendar ageing of lithium-ion batteries, J. Energy Storage 13 (2017) 176–183, http://dx.doi.org/10.1016/j.est.2017.06.009, URL https://www.sciencedirect.com/science/article/pii/S2352152X17300634.

[27] Y. Liu, K. Xie, Y. Pan, H. Wang, Y. Li, C. Zheng, Simplified modeling and parameter estimation to predict calendar life of Li-ion batteries, Solid State Ion. 320 (2018) 126–131, http://dx.doi.org/10.1016/j.ssi.2018.02.038, URL https://www.sciencedirect.com/science/article/pii/S0167273817308779.

[28] N. Shi, Z. Chen, M. Niu, Z. He, Y. Wang, J. Cui, State-of-charge estimation for the lithium-ion battery based on adaptive extended Kalman filter using improved parameter identification, J. Energy Storage 45 (2022) 103518, http://dx.doi.org/10.1016/j.est.2021.103518, URL https://www.sciencedirect.com/science/article/pii/S2352152X21011993.

[29] R. Mathieu, I. Baghdadi, O. Briat, P. Gyan, J.-M. Vinassa, D-optimal design of experiments applied to lithium battery for ageing model calibration, Energy 141 (2017) 2108–2119, http://dx.doi.org/10.1016/j.energy.2017.11.130, URL https://www.sciencedirect.com/science/article/pii/S0360544217319886.

[30] P. Gasper, K. Gering, E. Dufek, K. Smith, Challenging practices of algebraic battery life models through statistical validation and model identification via machine-learning, J. Electrochem. Soc. 168 (2) (2021) 020502, http://dx.doi.org/10.1149/1945-7111/abdde1.

[31] E. Thomas, I. Bloom, J. Christophersen, V. Battaglia, Rate-based degradation modeling of lithium-ion cells, J. Power Sources 206 (2012) 378–382, http://dx.doi.org/10.1016/j.jpowsour.2012.01.106, URL https://www.sciencedirect.com/science/article/pii/S0378775312002078.

[32] R. Mingant, M. Petit, S. Belaïd, J. Bernard, Data-driven model development to predict the aging of a Li-ion battery pack in electric vehicles representative conditions, J. Energy Storage 39 (2021) 102592, http://dx.doi.org/10.1016/j.est.2021.102592, URL https://www.sciencedirect.com/science/article/pii/S2352152X21003352.

[33] M. Lucu, E. Martinez-Laserna, I. Gandiaga, H. Camblong, A critical review on self-adaptive Li-ion battery ageing models, J. Power Sources 401 (2018) 85–101, http://dx.doi.org/10.1016/j.jpowsour.2018.08.064, URL https://www.sciencedirect.com/science/article/pii/S0378775318309297.

[34] K. Liu, Y. Li, X. Hu, M. Lucu, W.D. Widanage, Gaussian process regression with automatic relevance determination kernel for calendar aging prediction of lithium-ion batteries, IEEE Trans. Ind. Inf. 16 (6) (2020) 3767–3777, http://dx.doi.org/10.1109/TII.2019.2941747.

[35] M. Andre, K. Steiner, H. Walz, T. Soczka-Guth, D.U. Sauer, A retrospective on lithium-ion batteries, J. Power Sources 196 (12) (2011) 5349–5356, http://dx.doi.org/10.1016/j.jpowsour.2010.07.071.

[36] C. Zou, L. Zhang, X. Hu, Z. Wang, T. Wik, M. Pecht, A review of fractional-order techniques applied to lithium-ion batteries, lead-acid batteries, and supercapacitors, J. Power Sources 390 (2018) 286–296, http://dx.doi.org/10.1016/j.jpowsour.2018.04.033, URL https://www.sciencedirect.com/science/article/pii/S0378775318303768.

[37] X. Hu, H. Yuan, C. Zou, Z. Li, L. Zhang, Co-estimation of state of charge and state of health for lithium-ion batteries based on fractional-order calculus, IEEE Trans. Veh. Technol. 67 (11) (2018) 10319–10329, http://dx.doi.org/10.1109/TVT.2018.2865664.

[38] J. Sabatier, Fractional order models are doubly infinite dimensional models and thus of infinite memory: Consequences on initialization and some solutions, Symmetry 13 (6) (2021) http://dx.doi.org/10.3390/sym13061099, URL https://www.mdpi.com/2073-8994/13/6/1099.

[39] I. Podlubny, Fractional Differential Equations. an Introduction to Fractional Derivatives, Fractional Differential Equations, to Methods of their Solution and Some of their Applications, Academic Press, San Diego/London, 1999.

[40] I. Petras, Fractional-Order Nonlinear Systems. Modeling, Analysis and Simulation, Springer-Verlag, Berlin Heidelberg, 2011.

[41] J.A. López-Villanueva, S. Rodríguez Bolívar, Constant phase element in the time domain: The problem of initialization, Energies 15 (3) (2022) 792, http://dx.doi.org/10.3390/en15030792.

[42] M. Safari, C. Delacourt, Modeling of a commercial graphite/lifepo4 cell, J. Electrochem. Soc. 158 (5) (2011) A562, http://dx.doi.org/10.1149/1.3567007.